NONLINEAR GENERATION OF KINETIC-SCALE WAVES BY MAGNETOHYDRODYNAMIC ALFVÉN WAVES AND NONLOCAL SPECTRAL TRANSPORT IN THE SOLAR WIND

J. S. Zhao[1,3], Y. Voitenko[2], D. J. Wu[1], AND J. De Keyser[2]

[1] Purple Mountain Observatory, Chinese Academy of Sciences, Nanjing, China; js_zhao@pmo.ac.cn
[2] Solar-Terrestrial Centre of Excellence, Space Physics Division, Belgian Institute for Space Aeronomy, Ringlaan-3-Avenue Circulaire, B-1180 Brussels, Belgium

ABSTRACT

We study the nonlocal nonlinear coupling and generation of kinetic Alfvén waves (KAWs) and kinetic slow waves (KSWs) by magnetohydrodynamic Alfvén waves (MHD AWs) in conditions typical for the solar wind in the inner heliosphere. This cross-scale process provides an alternative to the turbulent energy cascade passing through many intermediate scales. The nonlinearities we study are proportional to the scalar products of wave vectors and hence are called "scalar" ones. Despite the strong Landau damping of kinetic waves, we found fast growing KAWs and KSWs at perpendicular wavelengths close to the ion gyroradius. Using the parametric decay formalism, we investigate two independent decay channels for the pump AW: forward decay (involving co-propagating product waves) and backward decay (involving counter-propagating product waves). The growth rate of the forward decay is typically 0.05 but can exceed 0.1 of the pump wave frequency. The resulting spectral transport is nonlocal and anisotropic, sharply increasing perpendicular wavenumbers but not parallel ones. AWs and KAWs propagating against the pump AW grow with about the same rate and contribute to the sunward wave flux in the solar wind. Our results suggest that the nonlocal decay of MHD AWs into KAWs and KSWs is a robust mechanism for the cross-scale spectral transport of the wave energy from MHD to dissipative kinetic scales in the solar wind and similar media.

Key words: instabilities – plasmas – solar wind – turbulence – waves

Online-only material: color figure

1. INTRODUCTION

Magnetohydrodynamic Alfvén waves (MHD AWs) permeate the solar atmosphere and the solar wind (Belcher & Davis 1971; Mathioudarks et al. 2012). These waves are thought to be produced by the convective motion jostling magnetic flux tubes below the photosphere and/or by the magnetic reconnections in the photospheric network (Ruzmaikin et al. 1998; Ryutova et al. 2001; Cranmer & van Ballegooijen 2005). There is ample observational evidence for MHD AWs in the chromosphere (De Pontieu et al. 2007; Cirtain et al. 2007; He et al. 2009; McIntosh et al. 2011), corona (Tomczyk et al. 2007; Okamoto et al. 2007; Tomczyk & McIntosh 2009), and solar wind (Belcher & Davis 1971). Recent observations of the transition region and solar corona have revealed a significant energy flux carried by the ubiquitous outward-propagating AWs, which is more than enough to heat the solar corona and to accelerate the fast solar wind (McIntosh et al. 2011). These waves are also thought to accelerate the slow solar winds and power the solar wind turbulence (Cranmer et al. 2007). However, how MHD AWs dissipate and deposit energy in the plasma of solar atmosphere and solar wind remains unresolved.

The inhomogeneous plasma density and flow in the solar atmosphere and solar wind support the phase mixing and resonance absorption of MHD AWs (Ionson 1978; Heyvaerts & Priest 1983; Voitenko & Goossens 2006), which evolve to small-scale kinetic Alfvén waves (KAWs) undergoing an efficient dissipation. The small dissipative AW scales can also be generated through the turbulent cascade mechanism in the AW turbulence resulting from nonlinear local interactions among counter-propagating AWs (Matthaeus et al. 1999; Cranmer &

van Ballegooijen 2003; Verdini & Velli 2007; van Ballegooijen et al. 2011). Modern theory of the AW turbulence suggests that KAWs are generated by the turbulent cascade at kinetic ion or electron scales (Howes et al. 2008, 2011; Voitenko & De Keyser 2011; Zhao et al. 2013), which is consistent with the turbulence characteristics measured in situ in the foreshock of the Earth and in the quiet solar wind (Sahraoui et al. 2009; Alexandrova et al. 2009). There is growing evidence that the proton kinetic scales (He et al. 2012; Roberts et al. 2013), as well as shorter ones (Chen et al. 2013), are dominated by KAWs (see also the overview of some measured KAW effects by Podesta 2013). Kinetic-wave–particle interactions of KAWs are efficient even in weakly collisional plasmas and in plasma heating and particle acceleration. These phenomena can be responsible for energy deposition by AWs in the solar atmosphere and solar wind (Cranmer & van Ballegooijen 2003; Wu & Fang 2003; Wu & Yang 2007; Chandran et al. 2010).

The above-mentioned processes imply a gradual evolution of wave energy from large MHD to small kinetic scales. At the same time, recent theory (Voitenko & Goossens 2005; Zhao et al. 2011a, 2011b) and simulations (Singh & Rao 2012) suggest that MHD waves can couple energy directly into small-scale kinetic waves. The first nonlocal decay of MHD-scale fast mode wave into KAWs was considered by Voitenko & Goossens (2002). Later, Voitenko & Goossens (2005) demonstrated analytically that the nonlocal decay of MHD AWs into KAWs should occur in very low-β plasmas where the gas/magnetic pressure ratio is less than the electron/proton mass ratio, $\beta < m_e/m_i$. This result was recently confirmed by numerical simulations (Singh & Rao 2012). A similar process, incorporating an oblique MHD AW as the pump wave, has been considered (Zhao et al. 2011a), and a fusion interaction between MHD AWs and KAWs has been studied in the low-β domain $m_e/m_i \ll \beta \ll 1$ (Zhao et al. 2011b). The advantage of the nonlocal decays as the spectral

---

[3] Also at Key Laboratory of Solar Activity, National Astronomical Observatories, Chinese Academy of Sciences, Beijing 100012, China.

transport mechanisms is that they transport energy in a single step across a wide interval of scales, avoiding many short local steps as, for example, in the local turbulence cascade (Howes et al. 2008; Zhao et al. 2013). Therefore, the nonlocal decays can provide faster spectral transport than the turbulence cascade or other gradual processes.

Formalism of parametric decay instability was first invented by Oraevsky & Sagdeev (1962) for electrostatic waves, which was then extended by Galeev & Oraevskii (1963) for electromagnetic MHD AWs. In the low-β plasma the strongest MHD decay (where all participating waves are MHD waves) was found into the backward propagating AW and forward slow wave (SW). The corresponding growth rate by Galeev & Oraevskii, γ_{GO}, can be estimated as

$$\frac{\gamma_{GO}}{\omega} \simeq \frac{1}{3\beta^{1/4}} \frac{B}{B_0}, \qquad (1)$$

where ω and B are the pump AW frequency and magnetic amplitude, respectively.

The process of the AW decay into the backward AW and forward SW has been confirmed by many subsequent analytical and simulation studies with various modifications (see recent papers by Nariyuki & Hada 2006; Matteini et al. 2010; Verscharen et al. 2012; Gao et al. 2013, Gao et al. 2014). The parametric decay is found in the hybrid simulations for both parallel and oblique AWs (Matteini et al. 2010; Verscharen et al. 2012; Gao et al. 2013, Gao et al. 2014), and AWs decay rapidly as the beam-induced oblique KAWs appear (Nariyuki et al. 2012). Simulations by Matteini et al. (2010) have shown that the ions can be accelerated by the magnetic-field-aligned electric field of the product SWs and can form the ion beams.

In the present paper, we keep leading-order nonlinear terms proportional to the scalar product $(\mathbf{k}_{0\perp} \cdot \mathbf{k}_{1\perp})$ of the pump and product wave vectors $\mathbf{k}_{0\perp}$ and $\mathbf{k}_{1\perp}$. These terms are responsible for the so-called "scalar" nonlinear interaction. In terms of the pump wave magnetic field $\mathbf{B}$ these terms are proportional to $(\mathbf{B} \times \mathbf{k}_{1\perp}) \cdot \hat{\mathbf{z}}$. The relevant nonlinear equations describing the scalar nonlinear interaction are derived below (Equations (26) and (27)). Some of these nonlinear terms, not accounted for in previous analytical studies, allowed us to capture a nonlocal MHD/kinetic decay of MHD AWs into kinetic-scale AWs and SWs. We show that in the low-β plasmas the MHD AWs can effectively excite KAWs and kinetic slow waves (KSWs) at small kinetic scales of about ion gyroradius ρ_i. In some cases, the MHD/kinetic decay can be more efficient than the MHD/MHD decay by Galeev & Oraevskii (1963) and generate dissipative KAWs and KSWs thus providing plasma heating and decreasing MHD AW amplitudes in the solar corona and solar wind. For example, it may contribute to the observed decrease of the wave amplitudes as the waves propagate from 1.1 $R_\odot$ to 1.4 $R_\odot$ in polar coronal holes (Bemporad & Abbo 2012; Hahn et al. 2012), and to KAW and KSW spectra observed in the solar wind turbulence (Howes et al. 2012; Klein et al. 2012) and in the terrestrial auroral zones (Wygant et al. 2002).

The outline of the paper is as follows. Section 2 presents a detailed derivation for the nonlinear coupling among low-frequency waves in the two-fluid plasma model. We then obtain the growth rate for KAWs and KSWs participating in the nonlinear decay MHD AW = KAW+KSW, where KAW can propagate either in the same direction as MHD AW or against it. In Section 3, a preliminary analysis is presented for these two decay channels in the non-dissipative case. It is shown that KAWs propagating against the MHD AW are generated at about

the same rate as the co-propagating KAWs. We further describe the model for the collisionless dissipation of KAWs and KSWs in Section 4, and investigate the nonlinear decay of MHD AWs into dissipative KAWs and KSWs in Section 5. In Section 6, we discuss our results in comparison to other studies, and present our conclusions in the final section, stressing the importance of the studied decay for the nonlocal spectral transport from MHD to kinetic scales in the solar wind.

2. TWO-FLUID MODEL

We start from the basic two-fluid and Maxwell equations, expanding all variables into the sum of background part plus perturbation: $A_0 + A$. Then the equations for the perturbations are

$$\partial_t \mathbf{v}_\alpha - \frac{q_\alpha}{m_\alpha} (\mathbf{E} + \mathbf{v}_\alpha \times \mathbf{B}_0) + \frac{1}{n_0 m_\alpha} \nabla P_\alpha = \mathbf{NLvel}_\alpha, \quad (2)$$

$$\partial_t n_\alpha + \nabla \cdot (n_0 \mathbf{v}_\alpha) = \mathrm{NLden}_\alpha, \qquad (3)$$

$$\nabla \times \mathbf{B} = \mu_0 \mathbf{J}, \qquad (4)$$

$$\nabla \times \mathbf{E} = -\partial_t \mathbf{B}, \qquad (5)$$

where we account for the nonlinear terms:

$$\mathbf{NLvel}_\alpha = -\mathbf{v}_\alpha \cdot \nabla \mathbf{v}_\alpha + \frac{q_\alpha}{m_\alpha} \mathbf{v}_\alpha \times \mathbf{B} + \frac{1}{n_0 m_\alpha} \frac{n_\alpha}{n_0} \nabla P_\alpha,$$

$$\mathrm{NLden}_\alpha = -\nabla \cdot (n_\alpha \mathbf{v}_\alpha),$$

and $\mathbf{v}_\alpha, n_\alpha, \mathbf{E}, \mathbf{B}$, and $\mathbf{J}$ are perturbations of the plasma velocity, number density, electric field, magnetic field, and current density, respectively; $q_\alpha, m_\alpha, T_\alpha$, and $P_\alpha = T_\alpha (n_0 + n_\alpha)^\gamma$ are particle charge, mass, temperature, and thermal pressure, respectively, for particle species α, i.e., $\alpha = i$ for the ions and $\alpha = e$ for the electrons; n_0 and B_0 are the background number density and magnetic field, respectively.

2.1. Derivation of General Nonlinear Equation

From the momentum equation (Equation (2)), the fluid velocity perturbation for the low-frequency waves where the wave frequency is much smaller than the ion cyclotron frequency can be expressed as

$$\mathbf{v}_{\alpha\perp} = \frac{1}{B_0 \omega_{c\alpha}} \partial_t \mathbf{E}_\perp + \frac{1}{B_0} \mathbf{E}_\perp \times \hat{\mathbf{z}} - \frac{\gamma T_\alpha}{m_\alpha \omega_{c\alpha}^2} \partial_t \nabla_\perp \frac{n_\alpha}{n_0}$$
$$- \frac{\gamma T_\alpha}{m_\alpha \omega_{c\alpha}} \nabla_\perp \frac{n_\alpha}{n_0} \times \hat{\mathbf{z}}$$
$$+ \frac{1}{\omega_{c\alpha}^2} \partial_t \mathbf{NLvel}_{\alpha\perp} + \frac{1}{\omega_{c\alpha}} \mathbf{NLvel}_{\alpha\perp} \times \hat{\mathbf{z}}, \qquad (6)$$

$$\partial_t v_{\alpha\parallel} = \frac{q_\alpha}{m_\alpha} E_z - \frac{\gamma T_\alpha}{m_\alpha} \partial_z \frac{n_\alpha}{n_0} + \mathbf{NLvel}_\alpha \cdot \hat{\mathbf{z}}, \qquad (7)$$

where $\omega_{c\alpha} \equiv q_\alpha B_0 / m_\alpha$ is the particle cyclotron frequency, and subscripts "$\parallel$" and "$\perp$" represent the perturbation parallel and perpendicular to the direction of the background magnetic field $\mathbf{B}_0 = B_0 \hat{\mathbf{z}}$.

By substituting Equations (6) and (7) into the following expression of the current density,

$$\mathbf{J} = n_0 e (\mathbf{v}_i - \mathbf{v}_e) + e n (\mathbf{v}_i - \mathbf{v}_e)$$
$$= n_0 e (\mathbf{v}_i - \mathbf{v}_e) + \frac{n}{n_0} \mathbf{J}, \qquad (8)$$

we obtain the perpendicular and parallel currents as

$$\mathbf{J}_\perp = \frac{n_0 m_i}{B_0^2} \partial_t \mathbf{E}_\perp - \frac{\gamma T_i}{B_0 \omega_{ci}} \partial_t \nabla_\perp n$$
$$- \frac{\gamma (T_i + T_e)}{B_0} \nabla_\perp n \times \hat{\mathbf{z}} + \mathbf{NLcur}_\perp, \qquad (9)$$

$$\partial_t J_\parallel = \frac{n_0 e^2}{m_e} E_z + \frac{e\gamma T_e}{m_e} \partial_z n + \mathrm{NLcur}_\parallel, \qquad (10)$$

with the nonlinear terms

$$\mathbf{NLcur}_\perp \equiv \frac{n_0 m_i}{B_0} \left[\left(\mathbf{NLvel}_{i\perp} + \frac{m_e}{m_i} \mathbf{NLvel}_{e\perp} \right) \times \hat{\mathbf{z}} \right.$$
$$\left. + \frac{1}{\omega_{ci}} \partial_t \left(\mathbf{NLvel}_{i\perp} - \frac{m_e^2}{m_i^2} \mathbf{NLvel}_{e\perp} \right) \right] + \frac{n}{n_0} \mathbf{J}_\perp,$$

$$\mathrm{NLcur}_\parallel \equiv n_0 e \left(\mathbf{NLvel}_i - \mathbf{NLvel}_e \right) \cdot \hat{\mathbf{z}} + \partial_t \left(\frac{n}{n_0} J_\parallel \right),$$

where the quasi-neutral condition has been used, $n_i = n_e \equiv n$. The same currents can also be expressed in terms of the electric field from Equations (3) and (4):

$$\mu_0 \partial_t \mathbf{J}_\perp = \nabla^2 \mathbf{E}_\perp - \nabla_\perp \left(\nabla \cdot \mathbf{E} \right), \qquad (11)$$

$$\mu_0 \partial_t J_\parallel = \nabla_\perp^2 E_z - \partial_z \nabla_\perp \cdot \mathbf{E}_\perp. \qquad (12)$$

By combining Equations (9)–(12), we get the coupled equations for electric field components:

$$\left(\partial_t^2 - V_A^2 \nabla^2 \right) \mathbf{E}_\perp + V_A^2 \nabla_\perp \nabla \cdot \mathbf{E} = \frac{\gamma T_i}{e} \partial_t^2 \nabla_\perp \frac{n}{n_0} + \frac{\gamma (T_i + T_e)}{e}$$
$$\times \omega_{ci} \partial_t \nabla_\perp \frac{n}{n_0} \times \hat{\mathbf{z}}$$
$$- \mu_0 V_A^2 \partial_t \mathbf{NLcur}_\perp, \quad (13)$$

$$\left(1 - \lambda_e^2 \nabla_\perp^2 \right) E_z + \lambda_e^2 \partial_z \nabla_\perp \cdot \mathbf{E}_\perp = - \frac{\gamma T_e}{e} \partial_z \frac{n}{n_0}$$
$$- \mu_0 \lambda_e^2 \mathrm{NLcur}_\parallel, \quad (14)$$

where V_A is the Alfvén speed and λ_e is the electron inertial length.

It is convenient to define a local coordinate system with three orthogonal unit vectors $\hat{\mathbf{e}}_p \equiv \nabla_\perp \times \hat{\mathbf{z}} / |\nabla_\perp|$, $\hat{\mathbf{e}}_t \equiv \nabla_\perp / |\nabla_\perp|$, and $\hat{\mathbf{z}}$. The corresponding electric field components E_p E_t and E_z can be expressed in terms of the normalized density perturbation n/n_0:

$$\left(\partial_t^2 - V_A^2 \partial^2 \right) E_p = \frac{\gamma (T_i + T_e)}{e} \omega_{ci} \partial_\perp \partial_t \frac{n}{n_0}$$
$$- \mu_0 V_A^2 \partial_t \mathbf{NLcur}_\perp \cdot \hat{\mathbf{e}}_p, \quad (15)$$

$$\left[\left(1 - \lambda_e^2 \partial_\perp^2 \right) \partial_t^2 - V_A^2 \partial_z^2 \right] E_t$$
$$= \left[\frac{\gamma T_e}{e} V_A^2 \partial_z^2 + \frac{\gamma T_i}{e} \left(1 - \lambda_e^2 \partial_\perp^2 \right) \partial_t^2 \right] \partial_\perp \frac{n}{n_0}$$
$$- \mu_0 V_A^2 \left(1 - \lambda_e^2 \partial_\perp^2 \right) \partial_t \mathbf{NLcur}_\perp \cdot \hat{\mathbf{e}}_t$$
$$+ \mu_0 \lambda_e^2 V_A^2 \partial_\perp \partial_z \mathrm{NLcur}_\parallel, \quad (16)$$

$$\left[\left(1 - \lambda_e^2 \partial_\perp^2 \right) \partial_t^2 - V_A^2 \partial_z^2 \right] E_z$$
$$= - \left[\frac{\gamma T_e}{e} \left(\partial_t^2 - V_A^2 \partial_z^2 \right) + \frac{\gamma T_i}{e} \lambda_e^2 \partial_\perp^2 \partial_t^2 \right] \partial_z \frac{n}{n_0}$$
$$+ \mu_0 V_A^2 \lambda_e^2 \partial_\perp \partial_z \partial_t \mathbf{NLcur}_\perp \cdot \hat{\mathbf{e}}_t$$
$$- \mu_0 \lambda_e^2 \left(\partial_t^2 - V_A^2 \partial_z^2 \right) \mathrm{NLcur}_\parallel. \quad (17)$$

The fourth complementing equation connecting n/n_0 to E_p, E_t, and E_z is derived from Equations (3), (6), and (7):

$$\left[\left(1 - \rho_i^2 \partial_\perp^2 \right) \partial_t^2 - V_{Ti}^2 \partial_z^2 \right] \frac{n}{n_0} = \frac{1}{B_0} \partial_\perp \partial_t E_p - \frac{1}{B_0 \omega_{ci}} \partial_\perp \partial_t^2 E_t$$
$$- \frac{e}{m_i} \partial_z E_z + \mathrm{NLden}_t, \quad (18)$$

where $\rho_i = (V_{Ti}/\omega_{ci})^{1/2}$ is the ion gyroradius, V_{Ti} and T_{Te} are, respectively, the ion and electron thermal velocities, and the nonlinear term is defined as

$$\mathrm{NLden}_t = - \frac{1}{\omega_{ci}} \partial_t \nabla \cdot \left(\frac{1}{\omega_{ci}} \partial_t \mathbf{NLvel}_{i\perp} + \mathbf{NLvel}_{i\perp} \times \hat{\mathbf{z}} \right)$$
$$- \partial_z \mathbf{NLvel}_i \cdot \hat{\mathbf{z}} + \frac{1}{n_0} \partial_t \mathrm{NLden}_i.$$

Using Equations (15)–(17), we can eliminate from Equation (18) all three components of the electric field, thus arriving to the general nonlinear equation for the low-frequency wave coupling in terms of n/n_0:

$$\left(\partial_t^2 - V_A^2 \partial^2 \right) \left[\left(1 - \lambda_e^2 \partial_\perp^2 \right) \partial_t^4 - V_A^2 \left(1 + \frac{\beta}{2} - \rho^2 \partial_\perp^2 \right) \partial_z^2 \partial_t^2 + V_A^2 V_T^2 \partial_z^4 \right] \frac{n}{n_0}$$
$$- V_T^2 \left[\left(1 - \lambda_e^2 \partial_\perp^2 \right) \partial_t^2 - V_A^2 \partial_z^2 \right] \partial_\perp^2 \partial_t^2 \frac{n}{n_0} =$$
$$- \frac{\mu_0 V_A^2}{B_0} \left[\left(1 - \lambda_e^2 \partial_\perp^2 \right) \partial_t^2 - V_A^2 \partial_z^2 \right] \partial_\perp \partial_t^2 \mathbf{NLcur}_\perp \cdot \hat{\mathbf{e}}_p$$
$$+ \frac{\mu_0 e V_A^2}{m_i} \left(\partial_t^2 - V_A^2 \partial^2 \right) \left[\frac{1}{\omega_{ci}^2} \left(1 - \lambda_e^2 \partial_\perp^2 \right) \partial_t^2 - \lambda_e^2 \partial_z^2 \right] \partial_\perp \partial_t \mathbf{NLcur}_\perp \cdot \hat{\mathbf{e}}_t$$
$$+ \frac{\mu_0 e \lambda_e^2}{m_i} \left(\partial_t^2 - V_A^2 \partial^2 \right) \left[\partial_t^2 - V_A^2 \left(\partial_z^2 + \frac{1}{\omega_{ci}^2} \partial_t^2 \partial_\perp^2 \right) \right] \partial_z \mathrm{NLcur}_\parallel$$
$$+ \left(\partial_t^2 - V_A^2 \partial^2 \right) \left[\left(1 - \lambda_e^2 \partial_\perp^2 \right) \partial_t^2 - V_A^2 \partial_z^2 \right] \mathrm{NLden}_t. \quad (19)$$

The definitions here are as follows :

$$V_T^2 = \frac{\gamma (T_i + T_e)}{m_i}, \quad \beta = \frac{2V_T^2}{V_A^2},$$
$$\rho^2 = \rho_i^2 + \rho_s^2 = \frac{\gamma T_i}{m_i \omega_{ci}^2} + \frac{\gamma T_e}{m_i \omega_{ci}^2}.$$

2.2. Linear and Nonlinear Responses of KAWs and KSWs in the Intermediate-β Plasmas

The general nonlinear equation (Equation (19)) describes the nonlinear dynamics of low-frequency wave modes: fast, slow, and Alfvén. In a specific plasma environment and for particular wave modes, the expression (Equation (19)) can be significantly simplified. Here we consider the nonlinear evolution of two plane waves, KAW$_1$ and KSW$_2$, with amplitudes $\propto \exp\left(i\mathbf{k}_{1,2} \cdot \mathbf{r} - i\omega_{1,2} t \right)$ in the low-β plasmas where both these waves are highly oblique, $k_\perp \gg k_z$. The wave properties of these two modes have previously been discussed in detail (see, e.g., Chen & Wu 2011a, 2011b, and references therein).

The fast wave decouples in this case and we retain only KAWs and KSWs.

Let us first consider the nonlinear equation (Equation (19)) for KAWs with $\omega \propto V_A k_z$. After the small terms of the order of $k_z^2/k_\perp^2$ and V_{Ti}^2/V_A^2 are neglected, the nonlinear equation reduces to

$$
\left[\partial_t^2 - V_A^2\left(1 - \rho^2\partial_\perp^2\right)\partial_z^2\right]\partial_\perp\partial_t^2\frac{n}{n_0}
$$
$$
= \frac{\mu_0}{B_0}\left(\partial_t^2 - V_A^2\partial_z^2\right)\partial_t^2\mathbf{NLcur}_\perp\cdot\hat{\mathbf{e}}_p + \frac{\mu_0 V_A^2}{B_0\omega_{ci}}\partial_\perp^2\partial_t^3\mathbf{NLcur}_\perp\cdot\hat{\mathbf{e}}_t
$$
$$
+ \frac{\mu_0 e\lambda_e^2}{m_i}\left[\left(1 - \lambda_i^2\partial_\perp^2\right)\partial_t^2 - V_A^2\partial_z^2\right]\partial_\perp\partial_z\mathrm{NLcur}_\parallel
$$
$$
+ \left(\partial_t^2 - V_A^2\partial_z^2\right)\partial_\perp\mathrm{NLden}_t. \tag{20}
$$

If we discard the nonlinear terms on the right-hand side of the last equation, the linear dispersion relation of KAWs is obtained:

$$
\omega^2 = V_A^2 k_z^2\left(1 + \rho^2 k_\perp^2\right). \tag{21}
$$

Then we can derive explicit expressions for the linear KAW response:

$$
\mathbf{v}_i = i\omega_{ci}\frac{1}{k_\perp}\frac{n}{n_0}\hat{\mathbf{e}}_p + \frac{\omega}{k_\perp}\frac{n}{n_0}\hat{\mathbf{e}}_t + V_T^2\frac{sk_z}{\omega}\frac{n}{n_0}\hat{\mathbf{z}},
$$
$$
\mathbf{v}_e = i\omega_{ci}\frac{\omega^2}{V_A^2 k_z^2}\frac{1}{k_\perp}\frac{n}{n_0}\hat{\mathbf{e}}_p - \frac{\beta}{2}\frac{\omega}{k_\perp}\frac{n}{n_0}\hat{\mathbf{e}}_t + \frac{s\omega}{k_z}\frac{n}{n_0}\hat{\mathbf{z}},
$$
$$
\mathbf{B} = -i\frac{B_0\omega_{ci}}{V_A^2}\frac{\omega}{k_\perp sk_z}\frac{n}{n_0}\hat{\mathbf{e}}_p + \frac{\beta B_0}{2}\frac{sk_z}{k_\perp}\frac{n}{n_0}\hat{\mathbf{e}}_t - \frac{\beta B_0}{2}\frac{n}{n_0}\hat{\mathbf{z}}, \tag{22}
$$

where $s = k_z/|k_z|$ denotes the propagation direction of the wave, such that $s = 1$ for the wave propagating in the direction of $\mathbf{B}_0$, and $s = -1$ for the waves propagating against $\mathbf{B}_0$.

For KSWs with $\omega \propto V_T k_z$, the nonlinear equation (Equation (19)) reduces to

$$
\left[\left(1 - \rho^2\partial_\perp^2\right)\partial_t^2 - V_T^2\partial_z^2\right]\partial_z^2\partial_\perp\frac{n}{n_0}
$$
$$
= \frac{\mu_0}{B_0}\partial_z^2\partial_t^2\mathbf{NLcur}_\perp\cdot\hat{\mathbf{e}}_p - \frac{\mu_0}{B_0\omega_{ci}}\partial_\perp^2\partial_t^3\mathbf{NLcur}_\perp\cdot\hat{\mathbf{e}}_t
$$
$$
+ \frac{\mu_0 e\lambda_e^2}{m_i}\left(\partial_z^2 + \frac{1}{\omega_{ci}^2}\partial_\perp^2\partial_t^2\right)\partial_\perp\partial_z\mathrm{NLcur}_\parallel + \partial_\perp\partial_z^2\mathrm{NLden}_t. \tag{23}
$$

Hence the linear dispersion relation for KSWs is

$$
\omega^2 = \frac{V_T^2 k_z^2}{1 + \rho^2 k_\perp^2}, \tag{24}
$$

and the linear response is given as follows:

$$
\mathbf{v}_i = -i\frac{V_T^2}{\omega_{ci}}k_\perp\frac{n}{n_0}\hat{\mathbf{e}}_p - \left(\rho^2 k_\perp^2 + \frac{\beta}{2}\right)\frac{\omega}{k_\perp}\frac{n}{n_0}\hat{\mathbf{e}}_t + V_T^2\frac{sk_z}{\omega}\frac{n}{n_0}\hat{\mathbf{z}},
$$
$$
\mathbf{v}_e = -i\frac{V_T^2}{\omega_{ci}}\frac{\omega^2}{V_A^2 k_z^2}k_\perp\frac{n}{n_0}\hat{\mathbf{e}}_p - \frac{\beta}{2}\frac{\omega}{k_\perp}\frac{n}{n_0}\hat{\mathbf{e}}_t
$$
$$
+ V_T^2\left(1 - \rho^2 k_\perp^2\frac{\omega^2}{V_T^2 k_z^2}\right)\frac{sk_z}{\omega}\frac{n}{n_0}\hat{\mathbf{z}},
$$
$$
\mathbf{B} = i\frac{\beta B_0}{2\omega_{ci}}\frac{sk_\perp\omega}{k_z}\frac{n}{n_0}\hat{\mathbf{e}}_p + \frac{\beta}{2}B_0\frac{sk_z}{k_\perp}\frac{n}{n_0}\hat{\mathbf{e}}_t - \frac{\beta}{2}B_0\frac{n}{n_0}\hat{\mathbf{z}}. \tag{25}
$$

2.3. Nonlinear Growth Rate of the Nonlocal Decay AW = KAW$_1$ + KSW$_2$

Here we study the nonlinear decay of MHD AWs into KAWs and KSWs. In what follows, the pump AW's parameters are without indices, KAW's parameters are with index "1," and KSW's parameters are with index "2." It is convenient to use the normalized magnetic $B_{1\perp}/B_0$ and density n_2/n_0 amplitudes as independent variables for KAWs and KSWs, respectively. The pump MHD AW is described by $B_\perp/B_0$ and propagates in the direction of B_0. Within approximations made in our study, the decay properties of the pump MHD AW propagating in the opposite direction are the same.

Then, using Equations (20)–(25) with scalar nonlinearities proportional to $[\mathbf{B}_\perp \times \mathbf{k}_{1\perp}]\cdot\hat{\mathbf{z}}$, the nonlinear dispersion equations are obtained for KAWs,

$$
\left[\omega_1^2 - V_A^2 k_{1z}^2\left(1 + \rho^2 k_{1\perp}^2\right)\right]\frac{B_{1\perp}}{B_0} = s_1\frac{\omega_1\omega}{2}\left(1 + \rho^2 k_{1\perp}^2\right)^{1/2}
$$
$$
\times \frac{[\mathbf{B}_\perp \times \mathbf{k}_{2\perp}]\cdot\hat{\mathbf{z}}}{k_{1\perp}B_0}\frac{n_2^*}{n_0}, \tag{26}
$$

and for KSW,

$$
\left(\omega_2^2 - \frac{V_T^2 k_{2z}^2}{1 + \rho^2 k_{2\perp}^2}\right)\frac{n_2}{n_0} = s_2\frac{\omega_2\omega}{2}\frac{V_A}{V_T}\frac{1 - s_1\left(1 + \rho^2 k_{1\perp}^2\right)^{1/2}\omega_1/\omega_0}{\left(1 + \rho^2 k_{1\perp}^2\right)\left(1 + \rho^2 k_{2\perp}^2\right)^{1/2}}
$$
$$
\times \frac{[\mathbf{B}_\perp \times \mathbf{k}_{1\perp}]\cdot\hat{\mathbf{z}}}{k_{1\perp}B_0}\frac{B_{1\perp}^*}{B_0}. \tag{27}
$$

Noting that $\mathbf{k}_{2\perp} \approx -\mathbf{k}_{1\perp}$ for the nonlocal interaction and combining the above equations, we obtain the growth rate of nonlinearly driven KAWs and KSWs:

$$
\gamma_{\mathrm{NL}}^2 = s_2\frac{\omega^2}{16}\frac{V_A}{V_T}\frac{\left(1 + \rho^2 k_{1\perp}^2\right)^{1/2} - s_1}{1 + \rho^2 k_{1\perp}^2}\frac{|[\mathbf{B}_\perp \times \mathbf{k}_{1\perp}]\cdot\hat{\mathbf{z}}|^2}{k_{1\perp}^2 B_0^2}, \tag{28}
$$

where s_1 and s_2 are the propagation directions of the product waves KAW$_1$ and KSW$_2$ with respect to the propagation direction of the pump wave AW ($s_\alpha = -1$ for the αth wave propagating against the pump and vice versa).

From dispersion relations (Equations (21) and (24)), one can see that the resonant conditions $\mathbf{k} = \mathbf{k}_1 + \mathbf{k}_2$ and $\omega = \omega_1 + \omega_2$ can be satisfied with forward KSW ($s_2 = 1$), but not with backward KSW ($s_2 = -1$). On the contrary, two decay channels involving forward ($s_1 = 1$) and backward ($s_1 = -1$) KAWs are allowed. Therefore, there are two possible decay channels for the MHD AW pump: (1) into forward KAW and KSW ($s_1 = s_2 = 1$), and (2) into backward KAW ($s_1 = -1$) and forward KSW ($s_2 = 1$). The corresponding parallelograms reflecting resonant conditions in the (ω, k_z) plane are presented in Figure 1.

3. PRELIMINARY ANALYSIS: DECAY INTO NON-DISSIPATIVE WAVES

The growth rate dependence on the perpendicular wavenumbers of the product kinetic waves is axially asymmetric because of the factor

$$
\gamma_{\mathrm{NL}}^2 \propto |\mathbf{k}_{1\perp} \times \mathbf{B}_\perp|^2 = k_{1\perp}^2 B_\perp^2 \sin^2\theta_1, \tag{29}
$$

where θ_1 is the angle between $\mathbf{k}_{1\perp}$ and $\mathbf{B}_\perp$. Therefore, the wave vectors of KAWs and KSWs generated by the scalar nonlinearities are elongated along the normal to the pump magnetic field, $\mathbf{k}_{1,2\perp} \perp \mathbf{B}_\perp$.
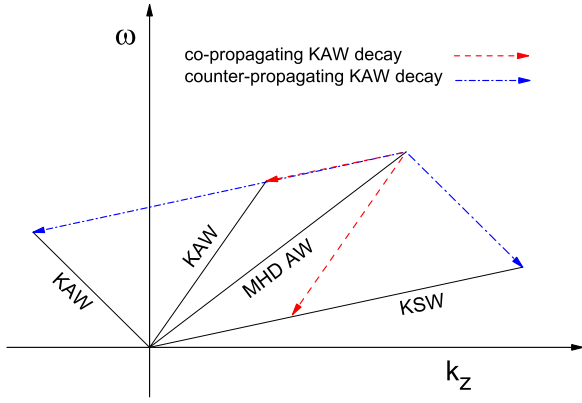
Figure 1. Two possible decay channels for the pump MHD AW: (1) into co-propagating KAW ($s_1 = 1$) and KSW ($s_2 = 1$), and (2) into counter-propagating KAW ($s_1 = -1$) and co-propagating KSW ($s_2 = 1$).

(A color version of this figure is available in the online journal.)

Substituting Equation (29) in Equation (28), we obtain the normalized nonlinear pumping rate

$$\frac{\gamma_{\rm NL}}{\omega} = \frac{\bar{\gamma}\,(s_1, \mu_1)}{4\beta^{1/4}} \left| \frac{B_\perp}{B_0} \right|, \qquad (30)$$

where $\mu_1 = \rho k_{1\perp} \simeq \rho k_{2\perp}$ is the normalized perpendicular wavenumber of the kinetic-scale waves, and

$$\bar{\gamma}\,(s_1, \mu_1) = \left(\frac{\left(1 + \mu_1^2\right)^{1/2} - s_1}{1 + \mu_1^2} \right)^{1/2},$$

is the profile function showing the wavenumber dependence of $\gamma_{\rm NL}$. The growth rate (Equation (30)) is already maximized with respect to the azimuthal angle θ_1 (the θ_1-dependence attains a maximum at $\theta_1 \simeq \pi/2$).

The profile function $\bar{\gamma}\,(s_1, \mu_1)$ has a maximum $\bar{\gamma}_{\rm m-} = \bar{\gamma}(-1, 0) = \sqrt{2}$ at $\mu_1 = \mu_{\rm m-} = 0$ for counter-propagating KAWs, which is actually a MHD limit where our results are consistent with the results by Galeev & Oraevskii (1963). For co-propagating AWs, the maximum $\bar{\gamma}_{\rm m+} = \bar{\gamma}(1, \sqrt{3}) = 1/2$ is attained at $\mu_1 = \mu_{\rm m+} = \sqrt{3}$. The pumping rate tends to zero in the limit $\mu_1 \to \infty$, where $\bar{\gamma} \to 0$ for both co- and counter-propagating product KAWs, $s_1 = \pm 1$.

The normalized pumping rate $\gamma_{\rm NL}/\omega$ as function of $\mu_{i1} = \rho_i k_{1\perp}$ ($= \mu_1/\sqrt{1 + T_e/T_i}$) is shown in Figure 2 for particular plasma and pump wave parameters. As is seen from Figure 2, at small μ_{i1} the nonlinear pumping rate for co-propagating KAWs first increases with increasing μ_{i1}, attains a maximum $\gamma_{\rm NL}/\omega \simeq 0.075$ at $\mu_{i1} \simeq 1.2$, and then gradually decays as μ_{i1} grows further. The pumping rate into counter-propagating KAW monotonously decreases starting from the maximum $\gamma_{\rm NL}/\omega \simeq 0.22$ at $\mu_{i1} = 0$. The scaling at large $\mu_{i1} \gg 1$ is the same in both cases, $\gamma_{\rm NL}/\omega \propto \mu_{i1}^{-1/2}$, and $\gamma_{\rm NL}(s_1 = -1) > \gamma_{\rm NL}(s_1 = 1)$ everywhere. $T_e/T_i = 1$ was assumed for the above estimations, and the behavior is similar to other values of T_e/T_i. The maximal pumping rate is decreased and shifted to lower μ_{i1} at the larger temperature ratio $T_e/T_i = 3$. For all values of T_e/T_i, the nonlinear pumping of energy into counter-propagating KAWs is somehow stronger than that into the co-propagating KAWs.

Summarizing the above results, in the case of weak or no dissipation, the pump AW will mainly generate resonant KAWs and KSWs in the vicinity of the above maxima. The resulting
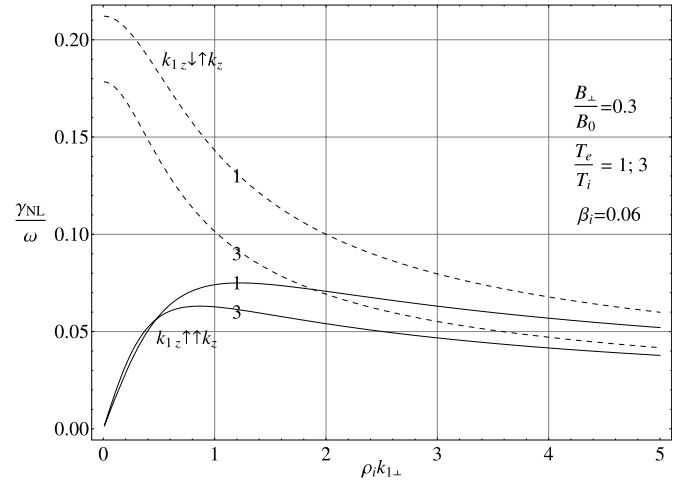
Figure 2. Relative nonlinear pumping rate of energy into KAWs and KSWs, $\gamma_{\rm NL}/\omega$, as function of the normalized wavenumber $\rho_i k_{1\perp}$. The nonlinear pumping rate into co-propagating KAWs ($s_1 = 1$) is shown by solid line, and into counter-propagating KAWs ($s_1 = -1$) is shown by the dashed line. The temperature ratio $T_e/T_i = 1$ and 3; the ion plasma beta $\beta_i = 0.06$. The nonlinear pumping into counter-propagating KAWs is two to three times stronger.

pumping rates per one wave period are

$$\frac{\gamma_{\rm NL\,max\,\pm}}{\omega} \simeq \frac{\bar{\gamma}_{\rm m\pm}}{4\beta^{1/4}} \frac{B_\perp}{B_0}. \qquad (31)$$

These fastest growing KAWs and KSWs determine the effective decay rate for the pump AW. At larger $\mu_{i1} > \mu_{\rm m\pm}$, the pumping rate $\gamma_{\rm NL\,max\,\pm}$ gradually decreases. Obviously, the nonlinear pumping rates are not very affected by β that comes with the power index 1/4, such that the coefficient $\beta^{1/4} \sim 1$ in the wide range $0.1 < \beta < 1$, in which case

$$\gamma_{\rm NL\,max} \sim \frac{\omega}{4} \frac{B_\perp}{B_0}.$$

Therefore, the most significant explicit influence of the pump wave parameters comes from the linear $\gamma_{\rm NL\,max}$ dependence of the pump magnetic amplitude $B_\perp$. With the pump wave amplitude $B_\perp/B_0 = 0.4$, we obtain a high growth rate $\gamma_{\rm NL\,max} \sim 0.1\omega$. Although the above relation indicates that the nonlinear decay of the MHD AW can occur even for very small $B_\perp$, the actual dissipation of kinetic waves imposes a decay condition $B_\perp > B_{\rm thr}$ with a finite threshold amplitude $B_{\rm thr}$, as is shown below. There are also implicit restrictions imposed by the small wave frequencies, which will be discussed below.

The total decay rate accounting for the damping of product waves γ_{L1} and γ_{L2} is

$$\gamma_{\rm tot} = \frac{\gamma_{L1} + \gamma_{L2}}{2} \pm \sqrt{\left(\frac{\gamma_{L1} - \gamma_{L2}}{2} \right)^2 + \gamma_{\rm NL}^2}, \qquad (32)$$

where $\gamma_{\rm NL}$ is given by Equation (30). To study nonlinear decay in weakly collisional plasmas, such as solar wind and magnetosphere, we must obtain expressions for damping rates of KAWs (γ_{L1}) and KSWs (γ_{L2}) in the kinetic plasma model. The analysis of the decay accounting for dissipative processes is given in the following sections.

4. COLLISIONLESS DISSIPATION OF KAWs AND KSWs

In the low-frequency domain, $\omega^2 \ll \omega_{ci}^2$, the dissipation is dominated by the Landau damping. The corresponding damping

rates for KAWs and KSWs can be presented as $\gamma_{L\alpha} = \omega_\alpha g_\alpha$, where $\alpha = 1$ for KAW, $\alpha = 2$ for KSW, and $g_\alpha = g_\alpha(\mu_i)$ depend only on the perpendicular wavenumber $\mu_i = \rho_i k_\perp$ but do not depend on other wave parameters. In Maxwellian plasmas, KAWs dissipate with the rate (see, e.g., Voitenko & Goossens 2006)

$$g_1(\mu) = -\sqrt{\frac{\pi}{8}} \frac{\mu_i^2}{K} \frac{T_e}{T_i} \frac{V_A}{V_{Ti}} \left(\frac{T_e}{T_i} \Lambda_0 \exp\left(-\frac{V_A^2 K^2}{2V_{Ti}^2}\right) \right.$$
$$\left. + \frac{V_{Ti}}{V_{Te}} \exp\left(-\frac{V_A^2 K^2}{2V_{Ti}^2} \frac{V_{Ti}^2}{V_{Te}^2}\right) \right), \qquad (33)$$

where $\Lambda_0 = I_0(\mu_i^2) \exp(-\mu_i^2)$, $I_0(\mu_i^2)$ is the zero-order Bessel function, $\mu_i^2 = (1 + T_e/T_i)^{-1}\mu^2$, and the KAW dispersion function $K \simeq \sqrt{1+\mu^2}$. The first term in $g_1(\mu_i)$ is due to ion Landau damping and the second term is due to electron Landau damping (effects of finite electron gyroradius are neglected).

For KSWs, we will use the low-frequency kinetic dispersion equation

$$1 + \sigma_e Z_e + \frac{T_e}{T_i}(1 - \Lambda_0) + \frac{T_e}{T_i}\Lambda_0 (1 + \sigma_i Z_i) = 0, \qquad (34)$$

obtained from the electrostatic approximation (right-hand side of Equation (5) by Voitenko & Goossens 2003). In Equation (34), $\sigma_\alpha = \omega/(\sqrt{2}k_z V_{T\alpha})$, and $Z_\alpha = Z(\sigma_\alpha)$ is the plasma dispersion function of the αth species. In order to find useful analytical expressions for KSW, it is customary to assume a non-isothermal plasma with $T_e/T_i \gg 1$ and expand Z_e (Z_i) in small σ_e (large σ_i) series, keeping first terms.

Unfortunately, there is no simple analytical solution $g_2(\mu_i)$ for KSWs in isothermal plasmas with $T_e \sim T_i$, which is the most interesting case. This is because the KSW phase velocity in this case is close to the ion thermal speed ($\sigma_i \sim 1$), and hence the plasma dispersion function $Z(\sigma_i)$ cannot be expanded in the large argument series. We therefore solved Equation (34) numerically and found the following fit to the numerical solution:

$$g_2(\mu_i) = 0.14 - 0.61\sqrt{\left(1 + \frac{T_i}{T_e}\right)\frac{0.42 + 0.58\mu_i^2}{0.42 + 0.038\mu_i^2} - 1} + 0.05$$
$$\times \left[\left(1 + \frac{T_i}{T_e}\right)\frac{0.42 + 0.58\mu_i^2}{0.42 + 0.038\mu_i^2} - 1\right]. \qquad (35)$$

Figure 3 presents the exact numerical solution of Equation (34) and its parametric fit (Equation (35)) for three values of the temperature ratio $T_e/T_i = 1/3$, 1, and 3. In the wide range of $\mu_{i2} = \rho_i k_{2\perp}$ from 0 to about 4, the fit and the numerical solution remain close to each other for the cases $T_e/T_i = 1$ and 3; they are closer with larger T_e/T_i. For the low-temperature ratio $T_e/T_i = 1/3$, the fit declines and the damping rate is underestimated at $\mu_{i2} > 2.5$. In general, with increasing $\rho_i^2 k_{1\perp}^2$, the KAW$_1$ Landau damping $|\gamma_{L1}|$ increases. Also, the KSW$_2$ phase velocity V_{ph2} decreases toward the thermal proton velocity making $|\gamma_{L2}|$ larger.

5. NONLINEAR GENERATION OF DISSIPATIVE KINETIC WAVES BY THE PARAMETRIC DECAY OF MHD AWs

For the co-propagating KAW decay, the collisionless damping of KAWs and KSWs suppresses the wave growth at large $\rho_i^2 k_{1\perp}^2 \gg 1$ and small $\rho_i^2 k_{1\perp}^2 \ll 1$, where the nonlinear pumping
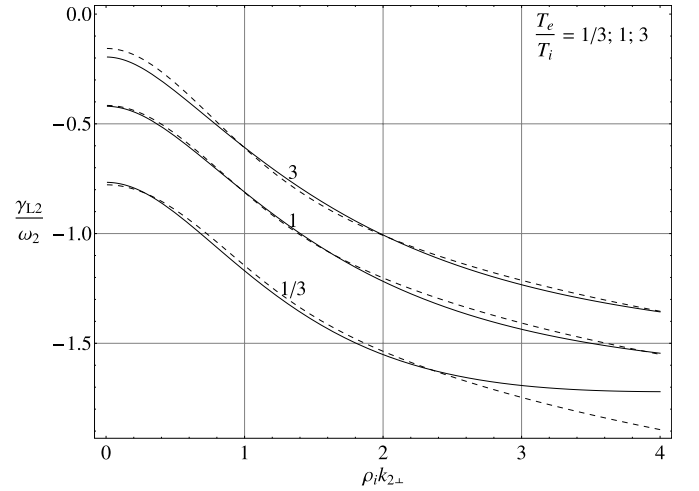
Figure 3. Numerical solution (dashed lines) of the kinetic dispersion equation for KSWs (Equation (34)) and the parametric fit (Equation (35)) (solid line) for the temperature ratios $T_e/T_i = 1/3$, 1, and 3.

drops faster than the linear damping. As a result, the nonlinear pumping can overcome the linear damping only in a limited region of perpendicular wavenumbers around $\rho_i^2 k_{1\perp}^2 \sim 1$. For the counter-propagating KAW decay, the collisionless damping exceeds the wave growth only at large $\rho_i^2 k_{1\perp}^2 \ll 1$. To find the perpendicular wavenumbers favorable for the wave growth, and the corresponding total growth rate, we rewrite Equation (32) in terms of g_1, g_2, and γ_{NL}:

$$\frac{\gamma_{tot}}{\omega} = \frac{f_1 g_1 + f_2 g_2}{2} \pm \sqrt{\left(\frac{f_1 g_1 - f_2 g_2}{2}\right)^2 + \frac{\gamma_{NL}^2}{\omega^2}}. \qquad (36)$$

In low-β plasmas, conditions of the spatio-temporal resonance fix frequencies of nonlinearly driven waves at

$$f_1 = \frac{\omega_1}{\omega} \simeq 1 - \frac{V_T}{V_A}\left(1 - \frac{s_1}{K}\right)\frac{1}{K},$$
$$f_2 = \frac{\omega_2}{\omega} \simeq \frac{V_T}{V_A}\left(1 - \frac{s_1}{K}\right)\frac{1}{K},$$

where s_1 is the sign of k_{1z}: $s_1 = 1$ for $k_{1z} > 0$ (co-propagating product KAW), $s_1 = -1$ for $k_{1z} < 0$ (counter-propagating KAW).

Expression (36) provides a basis for our further analysis of the total growth rate for the nonlocal decay AW = KAW + KSW, including collisionless dissipative effects. In what follows we will focus on the co-propagating KAW decay found in the present study.

In Figure 4, we first show the perpendicular wavenumber dependence $\gamma_{tot} = \gamma_{tot}(s_1 = 1, \rho_i k_{1\perp})$ in comparison to the nonlinear pumping rate γ_{NL}. The linear damping rates for KAWs (γ_{L1}) and for KSWs (γ_{L2}) are also shown for comparison. Note that all these rates are normalized by the pump wave frequency ω. It appears that the linear damping not only reduces the growth rate, but also shifts its maximum toward lower perpendicular wavenumbers $\rho_i k_{1\perp} \simeq \rho_i k_{2\perp}$ of the nonlinearly driven waves. The KSW damping is stronger near the maximum of the decay rate, but γ_{L1} becomes dominant at larger μ_{i1}, where γ_{L2} saturates (not shown). Another consequence of the wave dissipation is a significantly smaller wavenumber spectrum of the instability, γ_{tot}, compared to the wide spectrum of pumping γ_{NL}. In accordance with Equation (31), the MHD wave should generate kinetic-scale KAWs and KSWs at the rate $\gamma_{NL\,max} \approx 0.04\omega$.

6
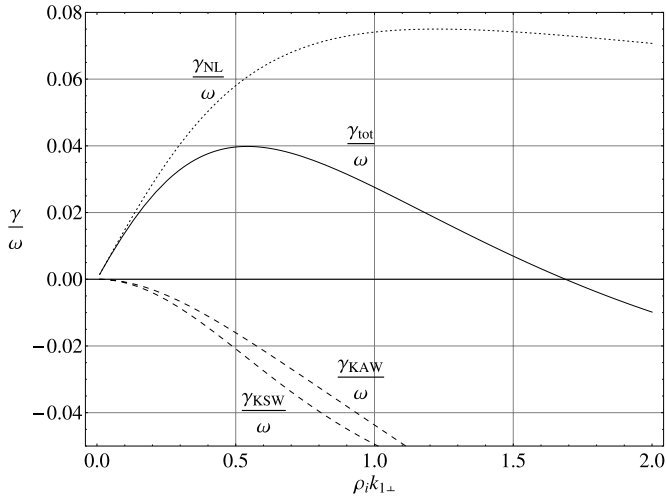
Figure 4. Total growth rate of the co-propagating KAWs, $\gamma_{\text{tot}}/\omega$, as function of normalized perpendicular wavenumber $\rho_i k_{1\perp}$ in the isothermal low-β plasma with $\beta_i = 0.06$ and $T_e = T_i$. The magnetic amplitude of the pump MHD AW is $B_\perp/B_0 = 0.3$. The nonlinear pumping rate γ_{NL} and Landau damping rates $\gamma_{\text{KAW}} = \gamma_{L1}$ and $\gamma_{\text{KSW}} = \gamma_{L2}$ of the nonlinearly generated KAWs and KSWs are also shown for reference.
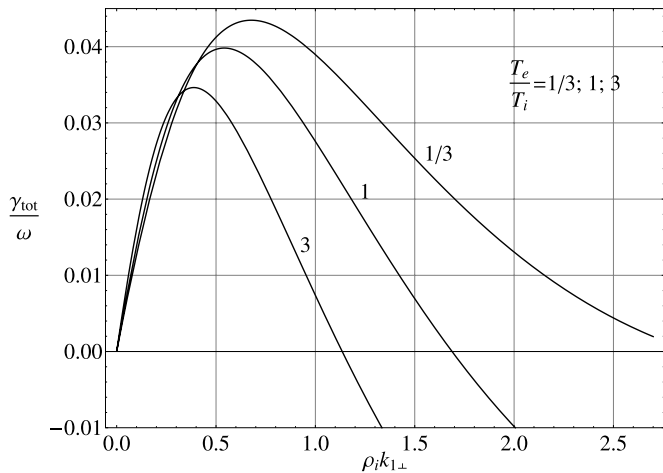
Figure 5. Total growth rate γ_{tot} of the co-propagating ($s_1 = 1$) product KAWs and KSWs as function of the normalized perpendicular wavenumber $\rho_i k_{1\perp}$. The plasma is low-β with $\beta_i = 0.06$ and isotropic, but T_e/T_i assumes three different values $T_e/T_i = 1/3$, 1, and 3. The MHD wave amplitude $B_\perp/B = 0.3$.

Next, we compare the growth rates of co-propagating KAWs for three different values of T_e/T_i (see Figure 5). The growth rate is larger for lower T_e/T_i, which results from the competition between stronger pumping and stronger damping at lower T_e/T_i. Again, the wavenumber spectra of the decay is significantly smaller because the damping suppresses the driving everywhere except for maximum.

Finally, we analyze behavior of the maximum growth rate $\gamma_{\text{max}} = \gamma_{\text{max}}(B_\perp/B_0, \omega, \beta_i, T_e/T_i)$, which is given by
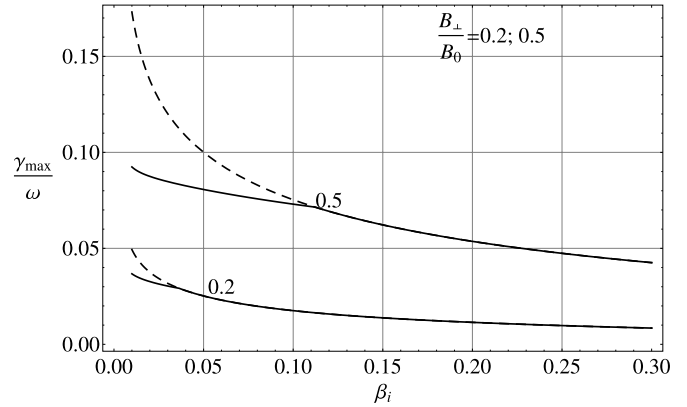
$$\gamma_{\text{max}} = \min[\gamma_{\text{m}}, \gamma_{\text{MD}}]. \tag{37}$$

Here

$$\gamma_{\text{m}} = \max_\mu[\gamma_{\text{tot}}(\mu)] \tag{38}$$

is the maximum attained by the growth rate $\gamma_{\text{tot}}(\mu)$ of the ordinary parametric decay, and

$$\gamma_{\text{MD}} \simeq 1.1\left(\frac{\omega_2}{\gamma_{\text{m}}}\right)^{1/3}\gamma_{\text{m}} \tag{39}$$

Figure 6. Maximum relative growth rates $\gamma_{\text{max}}/\omega$ of the co-propagating KAWs as functions of β_i at two MHD AW amplitudes $B_\perp/B_0 = 0.2$ and 0.5. The temperature ratio $T_e/T_i = 1$. In the bifurcation points, the decay switches to the regime of modified decay. The ordinary decay is shown for comparison by the dashed lines.

is the maximum growth rate of the modified parametric decay. In expressions (37)–(39), a modified decay formalism is taken into account. As explained by Oraevsky (1983), the modified decay formalism and the corresponding growth rate (Equation (39)) should be applied once the ordinary decay rate overcomes the lowest frequency participating in the decay. Since the lowest frequency in our case is the frequency of the product KSW, at $\gamma_{\text{m}} > \omega_2$ the actual growth rate becomes Equation (39).

It is convenient to normalize all γ's by the MHD AW frequency ω. The relative growth rate $\gamma_{\text{max}}/\omega$ is shown in Figure 6 as function of the ion plasma beta $\beta_i = 2V_{Ti}^2/V_A^2$. It is seen that the process enhances toward lower β_i and weakens toward higher β_i, but the overall difference is not very large.

As shown in Figure 6, there is a transition to the modified decay at low β_i where the dependence becomes more complex. The transition occurs when the ordinary growth rate becomes equal to the KSW frequency. The modified parametric decay operates in the pump frequency range below the transition frequency and causes the decay rate to decrease (the ordinary growth rate in this frequency range would be faster, as shown for comparison by the dashed lines). The ordinary decay operates at larger β_i.

Formally, one can find the decay threshold by setting $\gamma_{\text{max}} = 0$ and solving for B_{thr}/B_0. However, given the limited time of the MHD AW existence, as well as various decorrelation mechanisms, we decided to use a more realistic conventional threshold calculated at $\gamma_{\text{max}} = 0.01\omega$. This choice means that the process should be faster than 100 periods of the pump MHD AW. We consider how this threshold behaves by solving $\gamma_{\text{max}} = 0.01\omega$ for B_{thr}/B_0 and varying the ion plasma beta β_i. The result is shown in Figure 7. The electron/ion temperature ratio T_e/T_i reduces the threshold (hence enforce the decay) at $T_e/T_i > 1$, which is explained by the weakening of Landau damping.

6. DISCUSSION

It is instructive to compare our nonlocal MHD-kinetic decay (Equation (31)) into backward KAW and forward KSW with the local MHD decay (Equation (1)) involving backward AW and forward SW (Galeev & Oraevskii 1963). By taking the MHD limit $\rho_i k_{1\perp} \to 0$ in the kinetic growth rate (Equation (31)), we recover the MHD result (Equation (1)) by Galeev & Oraevskii (1963). The maximum is attained at $\rho_i k_{1\perp} = 0$, but the peak is
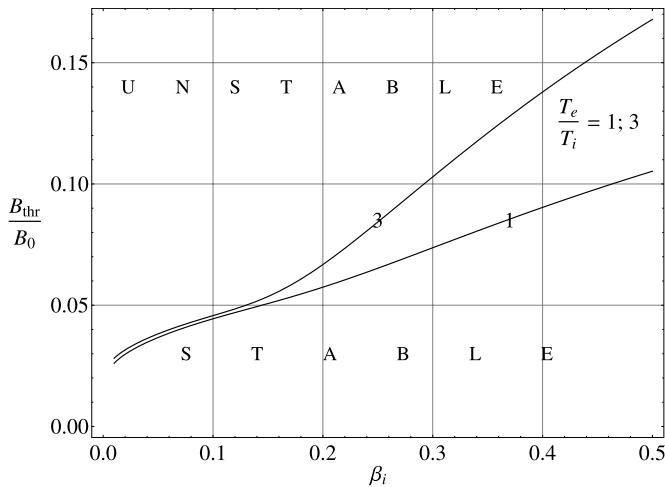
Figure 7. Conventional threshold of the co-propagating decay B_{thr}/B_0 calculated from the condition $\gamma_{max}(B_{thr}/B_0) = 0.01\omega$, as function of the ion plasma beta β_i. The threshold at lower $T_e/T_i = 1$ (solid lines) is lower than at $T_e/T_i = 3$.

not sharp and the growth rate of kinetic-scale waves at $\rho_i k_{1\perp} = 1$ is only by factor 0.7 smaller than at maximum.

On the contrary, the co-propagating decay develops fastest at $\rho_i k_{1\perp} \sim 1$, whereas its MHD counterpart does not exist. The co-propagating decay of MHD AWs is therefore intrinsically nonlocal and only generates kinetic waves. Although the (kinetic) co-propagating growth rate is formally almost three times smaller than the counter-propagating MHD one, the actual generation of kinetic waves is not necessarily weaker. For example, AWs in the solar wind usually have finite correlation lengths $l_z \sim \lambda_z \sim 2\pi/k_z$, which limits their linear correlation time and hence the time available for the waves to interact nonlinearly. In particular, the correlation time for counter-propagating AWs is at least two times shorter than for co-propagating AWs, which favors the co-propagating decay and can make it dominant. These effects related to linear decorrelation need further investigation (e.g., using the random phase approach).

The nonlinear generation of KAWs and KSWs by the Alfvénic pump wave has been previously studied by Hasegawa & Chen (1976). However, the pump AW considered by Hasegawa & Chen (1976) was already in the kinetic regime, i.e., it was a KAW. It is clear that the growth rate found by Hasegawa & Chen (1976) vanishes in the limit $k_\perp \rightarrow 0$, which means that only a local nonlinear interaction was captured. The same approximation has been used by many other authors (see, e.g., Brodin et al. 2006; Kryshtal' et al. 2007; Kumar & Sharma 2011), which did not allow them to capture the nonlocal interaction. We kept the nonlinear terms neglected by previous authors, which dominate at large $k_\perp$ of product waves and lead to the essentially nonlocal interactions.

Decay of parallel-propagating AWs into oblique Alfvén and density waves was recently observed in the two-dimensional hybrid simulations by Gao et al. (2013). We believe that Gao et al. have captured another decay, which is much slower than the nonlocal decay we study here. Indeed, with parameters used by Gao et al. in their run 1, our nonlocal decay would generate oblique product waves within the time scale $t\omega_{ci} < 1000$, well before the oblique waves appear in Figure 2 by Gao et al. (2013). Also, the perpendicular wavenumbers generated by our decay, $\rho_i k_{1\perp} \sim 1$, are much larger than those observed

in the simulations, $\rho_i k_{1\perp} \sim 0.01$. Waves with such large wavenumbers as ours ($\rho_i k_{1\perp} \sim 1$) could not be captured by these hybrid simulations because of their insufficient spatial resolution, limited by the ion inertial length.

In the present study, we are focused on the initial stage of the three-wave parametric decay where the parallel transport appears to be inefficient. Since this process cannot contribute to the small-scale parallel component observed by He et al. (2011) and Podesta & Gary (2011), other mechanism(s) should be involved. Recent simulations by Gao et al. (2014) suggest that this parallel component can be generated at the later stages when the modulation instability develops due to four-wave interactions.

The close analog of the process we study here is the nonlocal decay AW = KAW + KAW studied by Voitenko & Goossens (2005) at very low $\beta < m_e/m_i$. Similar to our decay, the decay considered by Voitenko & Goossens (2005) is efficient for parallel-propagating MHD AWs ($k_\perp = 0$) and is essentially nonlocal, generating highly oblique kinetic waves. There is, however, a principal difference: Voitenko & Goossens considered nonlinearities proportional to $k_{1\perp} \cdot B_\perp$, whereas we kept the terms $\propto k_{1\perp} \times B_\perp$. As a consequence, our decay generates $k_{1\perp} \perp B_\perp$, which is opposite to the case $k_{1\perp} \| B_\perp$ by Voitenko & Goossens. Magnetic polarization is also different: $B_{1\perp} \| B_\perp$ in our case, and $B_{1\perp} \perp B_\perp$ in the case by Voitenko & Goossens. In the near future, we plan to extend our investigation to include the nonlinearities $\propto k_{1\perp} \cdot B_\perp$.

Regardless of which decay dominates, the MHD AW spectrum with a preferred polarization direction should generate a spectrum of KAWs that are also polarized. The MHD AW anisotropy is indeed observed in the solar wind (Belcher & Davis 1971), and can either be a consequence of the sampling effect, or an inherent property of the MHD turbulence (Turner et al. 2012). However, we do not know of any correlation studies comparing simultaneously measured wave polarizations at MHD and kinetic scales, which would allow us to check if one of the above trends exists.

The fraction of the MHD wave energy that will be deposited into KAWs and KSWs via nonlocal coupling depends on the correlation times of MHD AWs. If the MHD pump waves keep their identity for a sufficiently long time, comparable to the nonlinear growth time of the kinetic waves, the nonlocal decay can be fulfilled in one single step and the related spectral transport is very efficient. This situation can be compared with the strong turbulence cascade but even more efficient because, in a single step, it transports energy over a much wider interval of scales. In the opposite situation, when the pump wave decorrelates faster than the kinetic waves grow, the nonlocal transport proceeds in many uncorrelated steps as in the weak turbulence. The more intermittent are local interactions among MHD AWs, the longer they exist, and hence the stronger is the direct nonlinear coupling of the MHD wave energy into kinetic scales.

Recent observations of the solar wind have revealed "standalone" AWs co-existent with the regular background MHD turbulence (Ghosh et al. 2009). These "standalone" AWs keep their coherency longer than the regular turbulent fluctuation because their spatio-temporal and amplitude proportions do not fit those of regular turbulent fluctuations and hence their nonlinear interaction with the background turbulence is inefficient. Simultaneous observations of such elevated AWs and KAWs at the proton gyroscale could help distinguishing the nonlocal transport we discuss here.

7. CONCLUSIONS

In the framework of parametric decay formalism, we investigated a nonlinear generation of small-scale KAWs and KSWs by large-scale MHD AWs. A new decay channel for MHD AW is found into forward kinetic-scale KAW and KSW. The previously known decay of MHD AW into backward MHD AW and forward MHD SW is extended to include the oblique kinetic regime. KAWs propagating against the pump MHD AW are generated at about the same rate as co-propagating KAWs and can contribute to the increasing fraction of the sunward waves as $k_{1\perp}$ approaches the ion gyroscale in the solar wind. The MHD decay by Galeev & Oraevskii (1963) is recovered by our counter-propagating kinetic decay in the MHD limit $\rho_i k_{1\perp} \to 0$. The collisionless dissipation (Landau damping) of the product KAWs and KSWs is strong and reduces their growth rate. Nevertheless, the MHD AWs with the parameters representative for the solar wind are efficient in generating small-scale KAWs and KSWs at $\rho_i k_{2\perp} \sim \rho_i k_{1\perp} \sim 1$. With reasonable MHD wave amplitudes $B \sim 0.3 B_0$, the growth rate of co-propagating kinetic waves can be quite high, $\gamma \sim 0.1\omega$, and can provide an efficient mechanism for the nonlocal spectral transport from MHD to kinetic scales.

The main features of the nonlocal MHD/kinetic decay into co-propagating waves and related spectral transport are as follows.

1. The nonlocal transport occurs in the cross-field direction such that the perpendicular wavenumbers of excited kinetic waves are much larger than the original wavenumbers of MHD AWs: $k_{2\perp} \simeq k_{1\perp} \gg k_{\perp}$. There is no nonlocal transport of the AW power in the parallel direction, $k_{1\parallel} \sim k_{\parallel}$.
2. The kinetic-scale KAWs and KSWs are most efficiently excited at the wavenumber $\rho_i k_{2\perp} \simeq \rho_i k_{1\perp} \lesssim 1$ defined by competition between the nonlinear pumping γ_{NL} and the counter-acting dissipation $\gamma_{L1,2}$.
3. Perpendicular wave vectors of nonlinearly generated kinetic waves tend to be normal to the pump magnetic field, $\mathbf{k}_{1\perp} \perp \mathbf{B}_{\perp}$.
4. The process is not sensitive to the pump perpendicular wavenumber $k_{\perp}$ and is efficient for the parallel-propagating MHD AWs, $k_{\perp} = 0$.
5. The high-frequency/high-amplitude MHD AWs are more efficient generators of kinetic waves than the low-frequency/low-amplitude ones. This property makes the process feasible for intermittent fluctuations arising in the solar wind turbulence at higher (but still MHD) frequencies.
6. The decay strengthens toward lower β, which could make it more efficient within 1 AU closer to the Sun where β is rapidly decreasing.

We believe that vectorial nonlinearities proportional to $[\mathbf{k}_{1\perp} \times \mathbf{k}_{\perp}] \cdot \hat{\mathbf{z}}$ can contribute to the nonlocal interaction as well and we are going to study them in the near future. One should note that the scalar and vectorial decays occupy different domains in the wave vector space, which makes their separate investigations possible.

REFERENCES

Alexandrova, O., Saur, J., Lacombe, C., et al. 2009, PhRvL, 103, 165003
Belcher, J. W., & Davis, L. 1971, JGR, 76, 3534
Bemporad, A., & Abbo, L. 2012, ApJ, 751, 110
Brodin, G., Stenflo, L., & Shukla, P. K. 2006, SoPh, 236, 285
Chandran, B. D. G., Li, B., Rogers, B. N., et al. 2010, ApJ, 720, 503
Chen, C. H. K., Boldyrev, S., Xia, Q., & Perez, J. C. 2013, PhRvL, 110, 225002
Chen, L., & Wu, D. J. 2011a, ChSBu, 56, 955
Chen, L., & Wu, D. J. 2011b, PhPl, 18, 072110
Cirtain, J. W., Golub, L., Lundquist, L., et al. 2007, Sci, 318, 1580
Cranmer, S. R., & van Ballegooijen, A. A. 2003, ApJ, 594, 573
Cranmer, S. R., & van Ballegooijen, A. A. 2005, ApJS, 156, 265
Cranmer, S. R., van Ballegooijen, A. A., & Edgar, R. J. 2007, ApJS, 171, 520
De Pontieu, B., McIntosh, S. W., Carlsson, M., et al. 2007, Sci, 318, 1574
Galeev, A. A., & Oraevskii, V. N. 1963, SPhD, 7, 988
Gao, X. L., Lu, Q. M., Li, X., Hao, Y., & Wang, S. 2014, ApJ, 780, 56
Gao, X. L., Lu, Q. M., Li, X., Shan, L. C., & Wang, S. 2013, PhPl, 20, 092106
Ghosh, S., Thomson, D. J., Matthaeus, W. H., & Lanzerotti, L. J. 2009, JGR, 114, A08106
Hahn, M., Landi, E., & Savin, D. W. 2012, ApJ, 753, 36
Hasegawa, A., & Chen, L. 1976, PhFl, 19, 1924
He, J. S., Marsch, E., Tu, C. Y., Yao, S., & Tian, H. 2011, ApJ, 731, 85
He, J. S., Tu, C. Y., Marsch, E., & Yao, S. 2012, ApJL, 745, L8
He, J. S., Tu, C. Y., Marsch, E., et al. 2009, A&A, 497, 525
Heyvaerts, J., & Priest, E. R. 1983, A&A, 117, 220
Howes, G. G., Bale, S. D., Klein, K. G., et al. 2012, ApJL, 753, L19
Howes, G. G., Cowley, S. C., Dorland, W., et al. 2008, JGR, 113, A05103
Howes, G. G., Tenbarge, J. M., & Dorland, W. 2011, PhPl, 18, 102305
Ionson, J. A. 1978, ApJ, 226, 650
Klein, K. G., Howes, G. G., TenBarge, J. M., et al. 2012, ApJ, 755, 159
Kryshtal', A. N., Sirenko, E. K., & Gerasimenko, S. V. 2007, KPCB, 23, 89
Kumar, S., & Sharma, R. P. 2011, JPlPh, 77, 237
Mathioudakis, M., Jess, D. B., & Erdélyi, R. 2013, SSRv, 175, 1
Matteini, L., Landi, S., Del Zanna, L., Velli, M., & Hellinger, P. 2010, GeoRL, 37, L20101
Matthaeus, W. H., Zank, G. P., Oughton, S., et al. 1999, ApJL, 51, L93
McIntosh, S. W., de Pontieu, B., Carlsson, M., et al. 2011, Natur, 475, 477
Nariyuki, Y., & Hada, T. 2006, PhPl, 13, 124501
Nariyuki, Y., Hada, T., & Tsubouchi, K. 2012, PhPl, 19, 082317
Okamoto, T. J., Tsuneta, S., Berger, T. E., et al. 2007, Sci, 318, 1577
Oraevsky, V. N. 1983, in Handbook of Plasma Physics, Basic Plasma Physics, Vol. 2, ed. A. A. Galeev & R. N. Sudan (Amsterdam: North-Holland), 37
Oraevsky, V. N., & Sagdeev, R. Z. 1962, Zh. Tekhn. Fiz., 32, 1291, (in Russian)
Podesta, J. J. 2013, SoPh, 286, 529
Podesta, J. J., & Gary, S. P. 2011, ApJ, 734, 15
Roberts, O. W., Li, X., & Li, B. 2013, ApJ, 769, 58
Ruzmaikin, A., & Berger, M. A. 1998, A&A, 337, L9
Ryutova, M., Habbal, S., Woo, R., & Tarbell, T. 2001, SoPh, 200, 213
Sahraoui, F., Goldstein, M. L., Robert, P., & Khotyaintsev, Y. V. 2009, PhRvL, 102, 231102
Singh, N., & Rao, S. 2012, PhPl, 19, 122303
Tomczyk, S., & McIntosh, S. W. 2009, ApJ, 697, 1384
Tomczyk, S., McIntosh, S. W., Keil, S. L., et al. 2007, Sci, 317, 1192
Turner, A. J., Gogoberidze, G., & Chapman, S. C. 2012, PhRvL, 108, 085001
van Ballegooijen, A. A., Asgari-Targhi, M., Cranmer, S. R., & DeLuca, E. E. 2011, ApJ, 736, 3
Verdini, A., & Velli, M. 2007, ApJ, 662, 669
Verscharen, D., Marsch, E., Motschmann, U., & Muller, J. 2012, PhRvE, 86, 027401
Voitenko, Y., & De Keyser, J. 2011, NPGeo, 18, 587
Voitenko, Y., & Goossens, M. 2002, SoPh, 209, 37
Voitenko, Y., & Goossens, M. 2003, SSRv, 107, 387
Voitenko, Y., & Goossens, M. 2005, PhRvL, 94, 135003
Voitenko, Y., & Goossens, M. 2006, SSRv, 122, 255
Wu, D. J., & Fang, C. 2003, ApJ, 596, 656
Wu, D. J., & Yang, L. 2007, ApJ, 659, 1693
Wygant, J. R., Keiling, C. A., Cattell, C. A., et al. 2002, JGR, 107, A1201
Zhao, J. S., Wu, D. J., & Lu, J. Y. 2011a, ApJ, 735, 114
Zhao, J. S., Wu, D. J., & Lu, J. Y. 2011b, PhPl, 18, 032903
Zhao, J. S., Wu, D. J., & Lu, J. Y. 2013, ApJ, 767, 109